BRIEF REPORT

Effects of Germline VHL Deficiency on Growth, Metabolism, and Mitochondria

Silverio Perrotta, M.D., Domenico Roberti, M.D., Ph.D., Debora Bencivenga, Ph.D., Paola Corsetto, Ph.D., Katie A. O'Brien, Ph.D., Martina Caiazza, M.S., Emanuela Stampone, Ph.D., Leanne Allison, B.Sc., Roland A. Fleck, Ph.D., Saverio Scianguetta, Ph.D., Immacolata Tartaglione, M.D., Ph.D., Peter A. Robbins, D.Phil., Maddalena Casale, M.D., Ph.D., James A. West, Ph.D., Clara Franzini-Armstrong, Ph.D., Julian L. Griffin, D.Phil., Angela M. Rizzo, Ph.D., Antonio A. Sinisi, M.D., Andrew J. Murray, D.Phil., Adriana Borriello, Ph.D., Federico Formenti, D.Phil., Ph.D., and Fulvio Della Ragione, M.D.

SUMMARY

Mutations in *VHL*, which encodes von Hippel–Lindau tumor suppressor (VHL), are associated with divergent diseases. We describe a patient with marked erythrocytosis and prominent mitochondrial alterations associated with a severe germline VHL deficiency due to homozygosity for a novel synonymous mutation (c.222C→A, p.V74V). The condition is characterized by early systemic onset and differs from Chuvash polycythemia (c.598C→T) in that it is associated with a strongly reduced growth rate, persistent hypoglycemia, and limited exercise capacity. We report changes in gene expression that reprogram carbohydrate and lipid metabolism, impair muscle mitochondrial respiratory function, and uncouple oxygen consumption from ATP production. Moreover, we identified unusual intermitochondrial connecting ducts. Our findings add unexpected information on the importance of the VHL–hypoxia-inducible factor (HIF) axis to human phenotypes. (Funded by Associazione Italiana Ricerca sul Cancro and others.)

Oxygen-sensing pathways orchestrate phenotypic adjustments from the cellular to the whole-body level, allowing function and survival under a variety of conditions.[1] The hypoxic response is exquisitely sensitive and dynamic, with relatively small changes in oxygen availability initiating transcriptional and post-transcriptional responses.[2] A fundamental process in this pathway is the ubiquitination and subsequent degradation of the hypoxia-inducible factors (HIFs), processes that are mainly regulated by the oxygen- and iron-dependent activity of the prolyl hydroxylase domain (PHD) enzymes and that require von Hippel–Lindau tumor suppressor (VHL).[3]

VHL encodes four different isoforms (pVHL-213, pVHL-160, pVHL-172, and pVHL-X1).[4] Mutations leading to *VHL* loss of function result in a number of diseases with divergent features.[5] These diseases include the VHL syndrome, an inherited disorder due to germline *VHL* alterations that lead to a predisposition to the development, on a somatic second hit, of a variety of tumors and fluid-filled sacs (cysts) in several body regions[6]; sporadic tumors, such as cerebellar hemangioblastomas, pheochromocytomas, and clear-cell renal-cell carcinoma[7,8]; and familial erythrocytosis type 2, caused by a biallelic germline *VHL* mutation (canonically c.598C→T [R200W], causing Chuvash polycythemia) that results in increased expression of HIF target genes.[9] Different sporadic *VHL* mutations have been reported[10] in addition to the canonical R200W mutation; some of these mutations are as-

From the Departments of Woman, Child, and General and Specialized Surgery (S.P., D.R., M. Caiazza, S.S., I.T., M. Casale), Precision Medicine (D.B., E.S., A.B., F.D.R.), and Advanced Medical and Surgical Sciences (A.A.S.), University of Campania Luigi Vanvitelli, Naples, and the Departments of Pharmacology and Biomolecular Science, University of Milan, Milan (P.C., A.M.R.) — both in Italy; the Departments of Physiology, Development, and Neuroscience (K.A.O., A.J.M.) and Biochemistry (J.A.W., J.L.G.), University of Cambridge, Cambridge, the Centre for Ultrastructural Imaging (L.A., R.A.F.) and the Centre for Human and Applied Physiological Sciences, Faculty of Life Sciences and Medicine (F.F.), King's College London, London, and the Department of Physiology, Anatomy, and Genetics (P.A.R., F.F.) and Nuffield Division of Anaesthetics (F.F.), University of Oxford, Oxford — all in the United Kingdom; and the Department of Cell and Developmental Biology, University of Pennsylvania, Philadelphia (C.F.-A.). Address reprint requests to Dr. Della Ragione at the Department of Precision Medicine, University of Campania Luigi Vanvitelli, via De Crecchio 7, Naples 80138, Italy, or at fulvio.dellaragione@unicampania.it; or to Dr. Formenti at the Centre for Human and Applied Physiological Sciences, Faculty of Life Sciences and Medicine, King's College London, London SE1 1UL, United Kingdom, or at federico.formenti@kcl.ac.uk.

Drs. Perrotta and Roberti and Drs. Formenti and Della Ragione contributed equally to this article.

N Engl J Med 2020;382:835-44.
DOI: 10.1056/NEJMoa1907362
Copyright © 2020 Massachusetts Medical Society.

The New England Journal of Medicine
Downloaded from nejm.org at the Bodleian Libraries of the University of Oxford on March 4, 2020. For personal use only. No other uses without permission.
Copyright © 2020 Massachusetts Medical Society. All rights reserved.

sociated with severe clinical phenotypes. For example, D126N caused fatal pulmonary hypertension in a homozygous patient.[11]

We present the clinical and molecular characterization of a case of familial erythrocytosis type 2 associated with a congenital, marked decrease in VHL levels. The patient had very early systemic onset of the disorder, with prenatal bradycardia and severe neonatal hypoglycemia. He underwent phlebotomy in his first days of life, and a polymorphic clinical phenotype developed. At the age of 12 years, he underwent clinical and genetic characterization that revealed homozygosity for a synonymous mutation in *VHL* (c.222C→A; p.V74V). The patient's genetic background and disease-related features stray from canonical familial erythrocytosis type 2[12] and suggest a new syndrome characterized by reduction in growth rate and pleiotropic alterations in energy metabolism, underpinned by marked mitochondrial dysfunction and structural changes.

CASE REPORT

The index patient, a son of healthy consanguineous white Italian parents (Fig. S1A in Supplementary Appendix 1, available with the full text of this article at NEJM.org; note that all supplementary figures and tables are located in Supplementary Appendix 1) was born by emergency cesarean section on evidence of prenatal bradycardia episodes. At birth, the index patient had severe hypoglycemia, which was treated with hydrocortisone for 1 month, and persistent bradycardia (Table 1). No signs of sepsis were detected. He received phototherapy for early neonatal jaundice and underwent phlebotomy when he was a few days old for hemoglobin and hematocrit values higher than the 99th percentile for his age.

A few months after birth, he began to show a marked failure to thrive and was administered recombinant growth hormone for 4 to 6 weeks, with no signs of growth hormone deficiency itself. Owing to the persistent hypoglycemia, he was treated with diazoxide for 3 years, which normalized his fasting glucose levels. When he was 12 years old, the patient was admitted to the University of Campania Hospital, Naples, Italy, with several phenotypic and metabolic abnormalities (Table 1), together with an abnormal cardiac rhythm, which manifested as bigeminal and trigeminal pulses and supraventricular premature beats (not judged as requiring treatment). At the age of 13 years, his height and growth velocity were 3.0 SD below the normal population mean for his sex and age; growth hormone–releasing hormone (GHRH) and arginine-stimulation testing produced a growth hormone (GH) peak of 33.6 ng per milliliter (a normal response is in the mid-60s in this age group), highlighting impairment in the GHRH–growth hormone–insulin-like growth factor 1 (IGF1) pathway. He underwent therapy with recombinant human IGF1, starting at a dose of 0.04 mg per kilogram of body weight and increasing to a full dose of 0.12 mg per kilogram. His growth velocity increased by 50% in 4 months, and he reached a height of 159 cm, with his genetic target being 162 to 178 cm (Fig. S1B). The patient is currently 22 years old.

He has undergone periodic phlebotomies of 5 to 7 ml per kilogram since he was a few days old (lately every 3 to 4 weeks). Although described as detrimental in patients with Chuvash polycythemia,[13] phlebotomy is currently the main prophylactic treatment[14] for symptoms such as severe headache and muscle cramps, possibly because of blood hyperviscosity. The pleiotropic effects of iron deficiency[15] demand strict control of iron bioavailability: iron supplementation (80 mg of ferrous sulfate per day), implemented since the patient was 14 years old, produced normal cellular iron availability (total iron-binding capacity, 402 μg per deciliter [72 μmol per liter]). The patient's parents were similar to controls with respect to clinical and laboratory measures (not shown).

METHODS

OVERSIGHT

This study was approved by the institutional review board of the University of Campania Luigi Vanvitelli. The patient and his parents provided written informed consent.

GENETIC ANALYSES

The genetic and protein analyses were performed on peripheral-blood mononuclear cells (PBMCs). *VHL* exons were amplified by polymerase chain reaction (PCR) and sequenced. *VHL* messenger RNA (mRNA) was quantified by reverse-transcriptase–quantitative PCR (RT-qPCR). Expression of hypoxia-dependent genes was investigated with a comprehensive array RT^2 Profiler PCR Array Human Hypoxia Signaling Path-

The New England Journal of Medicine
Downloaded from nejm.org at the Bodleian Libraries of the University of Oxford on March 4, 2020. For personal use only. No other uses without permission.
Copyright © 2020 Massachusetts Medical Society. All rights reserved.

way (Qiagen). Transcription levels of selected genes were confirmed by RT-qPCR. Immunoblotting was used to analyze protein levels. Whole-genome sequencing and bioinformatics analyses were performed by Admera Health.

FUNCTIONAL AND LABORATORY STUDIES

Respirometry analyses were performed on muscle fibers. The in vivo phenotype of the index patient was characterized by investigating exercise capacity and cardiopulmonary responses to acute hypoxia (end-tidal partial pressure of oxygen, 50 mm Hg).

Blood and red-cell membrane lipids were studied by means of high-performance liquid chromatography and gas chromatography. Muscle metabolites were analyzed by ultra-high-performance liquid chromatography–mass spectrometry. Muscle ultrastructure was studied with transmission electron microscopy. Additional methodologic details, including details of the methods used to evaluate glycemia, are provided in Supplementary Appendix 1.

RESULTS

MUTATIONAL ANALYSIS AND TRANSCRIPTIONAL AND BIOCHEMICAL CHARACTERIZATION

Direct sequencing of the exons and exon–intron boundaries of the *VHL* gene revealed homozygosity for a novel mutation causing a synonymous variation, p.V74V (c.222C→A) (Fig. 1A). To support the identification of pathogenic *VHL* mutations and to investigate the occurrence of other possible pathologic genetic variants, whole-genome sequencing of the patient and his parents was performed (Supplementary Appendix 1). Three groups of mutations were highlighted: mutations for which the patient was homozygous and his parents were simple heterozygous (Supplementary Appendix 2), mutations for which the patient was homozygous and the parents were compound double heterozygous (Supplementary Appendix 3), and mutations for which the patient was double heterozygous, with one mutation inherited from the heterozygous mother and one inherited from the heterozygous father (Supplementary Appendix 4).

A total of 249,010 mutations were identified, with only 1134 (0.46%) being exonic (Fig. S1C). As discussed in Supplementary Appendix 1, the use of predictive software for identifying damaging mutations or for pathway analysis identi-

Table 1. Clinical and Laboratory Measures.*

Measure	Value in Patient	Reference Range
At birth		
Hematocrit (%)	73	42–64
Hemoglobin (g/dl)	22.5	14–19.9
Glucose (mg/dl)	24	45–100
17-Hydroxyprogesterone (μg/liter)	55	0.7–43
Insulin (μU/ml)	1.28	2.42–13
Heart rate (beats/min)	85	120–160
At genetic diagnosis (12 yr of age)		
Hematocrit (%)	62	35–46
Hemoglobin (g/dl)	19.8	12.2–15.4
Erythropoietin (mU/ml)	496	1.6–34
Ferritin (ng/ml)	6	20–150
GHRH+arginine test, GH peak (ng/ml)	33.6	5–12
Height (cm)	132.3†	
Glucose (mg/dl)	42	60–100
Blood pressure (mm Hg)	75/35‡	
Venous lactate (mmol/liter)	2.3	<1
Arterial blood gas analysis		
pH	7.41	7.38–7.42
pCO_2 (mm Hg)	24.8	35–45
pO_2 (mm Hg)	121	83–105
$cHCO_3^-$ (mmol/liter)	15.6	22–26
cBASE (mmol/liter)	–8.1	–2 to 2
At 22 yr of age		
Hematocrit (%)	55.5	37–49
Hemoglobin (g/dl)	17.5	12.5–16.5
Reticulocyte count (cells/μl)	175,000	
Ferritin (ng/ml)	18	20–150
Total iron-binding capacity (μg/dl)	402	240–450
Insulin (μU/ml)	3.5	3–8
Glucose (mg/dl)	49	60–100
Cholesterol (mg/dl)	95	60–200
HDL cholesterol (mg/dl)	31	>35
LDL cholesterol (mg/dl)	55	<129
Total cholesterol:HDL cholesterol ratio	3.13	

* The main anomalous clinical and laboratory measures at each indicated age are shown. Reference values are the normal values for age and sex. The patient has been treated with monthly phlebotomies, iron supplementation, and periodic antihistaminic treatments. To convert the values for cholesterol to millimoles per liter, multiply by 0.02586. To convert the values for glucose to millimoles per liter, multiply by 0.05551. To convert the values for iron-binding capacity to micromoles per liter, multiply by 0.1791. To convert the values for insulin to picomoles per liter, multiply by 6.945. The term cBASE denotes base excess in blood, $cHCO_3^-$ concentration of bicarbonate, GH growth hormone, GHRH growth hormone–releasing hormone, HDL high-density lipoprotein, LDL low-density lipoprotein, pCO_2 partial pressure of carbon dioxide, and pO_2 partial pressure of oxygen.

† The patient's height was 3 SD below the population mean for his age and sex.

‡ The patient's systolic blood pressure was 2 SD below the mean for his age and sex; his diastolic blood pressure was in the 3rd percentile for his age and sex.

The New England Journal of Medicine
Downloaded from nejm.org at the Bodleian Libraries of the University of Oxford on March 4, 2020. For personal use only. No other uses without permission.
Copyright © 2020 Massachusetts Medical Society. All rights reserved.

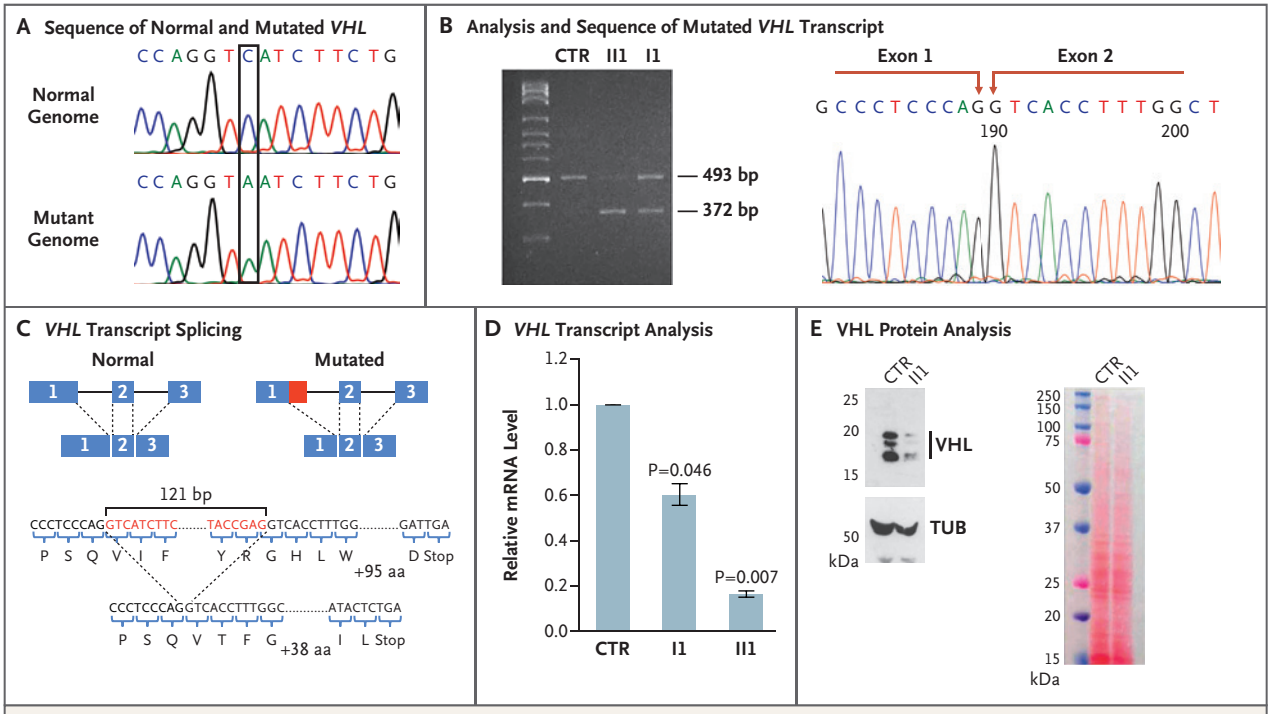

Figure 1. Effects of the Mutation on VHL Levels.

Panel A shows a sequence chromatogram for *VHL*, which encodes von Hippel–Lindau tumor suppressor (VHL); the normal and mutated genome are shown, highlighting (in the box) the homozygous mutation at nucleotide 222 (C→A). The identified mutation affects *VHL* transcript maturation, since it creates an alternative donor site and causes a 121-bp loss of *VHL* mature RNA transcript. Panel B shows electrophoretic analysis of reverse-transcriptase–polymerase-chain-reaction (RT-PCR) products with primers designed against exons 1 and 2 (lane 1, molecular weight marker; lane 2, control participant [CTR]; lane 3, index patient [II1]; lane 4, index patient's father [I1]). The sequence chromatogram shows the anomalous short band (372 bp) with 121-bp loss. Panel C shows normal and mutated *VHL* messenger RNA (mRNA) splicing, illustrating the reduction of exon 1. Altered splicing caused a shift in the open reading frame and originates a premature stop codon. Panel D shows quantification of *VHL* mRNA in a control, the father of the index patient, and the index patient, from an analysis of a specific exon 2 region. Quantitative RT-PCR (RT-qPCR) was performed on total peripheral-blood mononuclear cell (PBMC) mRNA. Mean values from three independent evaluations are shown and are expressed as the ratio of the mRNA level in the patient to that in the control; I bars indicate the standard deviation. P values are for the comparison with control. Panel E shows Western blot analysis of VHL protein isoforms in PBMCs from a control and from the patient. VHL antibodies were directed against an epitope occurring in normal and mutated VHL. Tubulin (TUB) is a control for loading. The filter stained with ponceau red is shown to confirm equal loading.

fied no variation that was clearly related to the patient's phenotype (Supplementary Appendixes 5 and 6). The c.222C→A change created a cryptic donor splicing site at nucleotide position 220 (NetGene2 and FSPLICE). RNA was analyzed to characterize the effect of the c.222C→A change on splicing. Primers annealing on exons 1 and 2 of the *VHL* complementary DNA (cDNA) were designed to produce a 493-bp amplicon. A *VHL* RT-PCR analysis revealed an additional band of 372 bp in the patient (II1 in Fig. 1B). The patient's father (I1) had a smaller amount of the anomalous transcript, and a control had only the longer transcript. Sequence analysis showed that the aberrant transcript was missing 121 bp, from nucleotide 220 to 340 (Fig. 1B). The aberrant splicing led to a shorter exon 1, causing a frameshift with an anomalous stop codon, which would in theory produce a shorter protein (Fig. 1C).

The full-length *VHL* mRNA levels in the patient and his father were approximately 80% and 40% lower, respectively, than those in a control participant (Fig. 1D). Levels of the three main VHL protein isoforms (pVHL-213, pVHL-160, and pVHL-172) were clearly reduced (Fig. 1E), suggesting impairment in VHL-dependent functions. Correspondingly, the HIF-1α nuclear immunofluorescence signal in the patient's lymphocytes was strongly enhanced as compared with that in a healthy control (Fig. S1D). According to the American College of Medical Genetics and Ge-

The New England Journal of Medicine
Downloaded from nejm.org at the Bodleian Libraries of the University of Oxford on March 4, 2020. For personal use only. No other uses without permission.
Copyright © 2020 Massachusetts Medical Society. All rights reserved.

nomic Guidelines, the c.222C→A *VHL* mutation can be classified as likely to be pathogenic, satisfying one strong and two moderate criteria.[16] The genetic change has been deposited in ClinVar repository under the accession number SCV000924583.

EXERCISE CAPACITY AND CARDIOPULMONARY RESPONSES TO ACUTE HYPOXIA

The patient had serious hypotension at diagnosis (blood pressure, 75/35 mm Hg), a condition not described in other forms of familial erythrocytosis, including classical familial erythrocytosis type 2, type 3 (due to *PHD2* loss of function), and type 4 (due to *HIF2A* gain of function).[17] To evaluate the phenotype associated with the genetic mutation, the patient's exercise capacity and response to hypoxic cardiopulmonary stress were tested with standard procedures.[18] The patient had elevated arterial partial pressure of oxygen, reduced arterial partial pressure of carbon dioxide, and reduced arterial bicarbonate (Table 1). At baseline while he was breathing ambient air, the patient's end-tidal partial pressure of oxygen was high, the end-tidal partial pressure of carbon dioxide was low, and the respiratory quotient was 0.803; this altered ventilatory control has been observed in Chuvash polycythemia[19] and mimics acclimatization to high-altitude hypoxia, overall suggesting the central role of the VHL–HIF pathway in the calibration of cardiopulmonary system physiology. The precise mechanisms underpinning altered ventilation remain to be elucidated. However, a study involving a mouse model of Chuvash polycythemia showed the occurrence of carotid-body hyperplasia and enhanced sensitivity to hypoxia.[20]

End-tidal partial pressure of oxygen and carbon dioxide were accurately controlled throughout the acute hypoxia exposure protocol; in particular, end-tidal partial pressure of carbon dioxide was controlled to reflect values observed at rest and from the arterial blood gas analysis (Fig. 2A). The patient's pulmonary arterial systolic pressure and cardiac output were elevated at baseline and increased markedly in response to hypoxia, similar to findings in patients with Chuvash polycythemia.[21]

The patient had a limited exercise capacity, associated with a low peak level of lactate in venous blood (Fig. 2B). Moreover, he had a greater than normal increase in ventilation for equivalent work rates, while end-tidal partial pressure of carbon dioxide remained low throughout the exercise protocol (Fig. 2B). These integrative aspects of the phenotype associated with the mutation in this patient partly recapitulate those described in Chuvash polycythemia.[21]

CHANGES IN GENE EXPRESSION AND MITOCHONDRIAL ALTERATIONS

In contrast to findings in patients with Chuvash polycythemia,[22] markedly altered expression of several HIF target genes was found in the analysis of RNA from the patient's PBMCs (Fig. 2C and Supplementary Appendix 1). *IGFBP3* (encoding insulin-like growth factor–binding protein 3) RNA levels were 80% lower than in either patients with Chuvash polycythemia or healthy controls (Fig. S1E). Lower *IGFBP3* expression has been reported in conditions under which activity of the GH–IGF1 axis is reduced.[23]

BNIP3L and *MXI1* are two key mitochondria-modulating genes. BNIP3L is a receptor accountable for stress-induced mitophagy,[24] and MXI1 is a negative transcriptional regulator of *MYC*, which is involved in mitochondrial biogenesis and metabolism.[25] RT-qPCR analysis showed that expression of *BNIP3L* and *MXI1* was more than 25 and 45 times as high, respectively, in our patient as in two controls, whereas there was no significant difference between the controls and two patients with Chuvash polycythemia with Italian heritage who were matched to our index patient for hematologic and iron measures (Fig. 2D). *BNIP3L*, *MXI1*, and *IGFBP3* expression in the patient's parents did not differ from that in controls (not shown). *BNIP3L* and *MXI1* expression was previously found to be enriched to a minor degree in a cohort of Russian patients with Chuvash polycythemia (1.31 and 1.18 times as high as normal, respectively), with low ferritin levels positively correlating with expression.[22] *BNIP3L* and *MXI1* up-regulation in our patient was confirmed at the protein level, suggesting marked mitochondrial dysfunction (Fig. 2E). Given the degree of these alterations that were found in the patient but were absent in patients with canonical familial erythrocytosis type 2, we investigated skeletal muscle mitochondrial function and morphology in vastus lateralis biopsy specimens.

Mitochondrial respiratory function was assessed in saponin-permeabilized muscle fibers with the use of high-resolution respirometry.[26] This revealed a marked suppression in the pa-

The New England Journal of Medicine
Downloaded from nejm.org at the Bodleian Libraries of the University of Oxford on March 4, 2020. For personal use only. No other uses without permission.
Copyright © 2020 Massachusetts Medical Society. All rights reserved.

A Cardiopulmonary Responses to Acute Hypoxia

Value	Baseline		Hypoxia	
	Patient	Control	Patient	Control
End-tidal O_2 (mm Hg)	120±5	100±4	46±1	50±1
End-tidal CO_2 (mm Hg)	25±3	39±3	28±1	39±2
PASP (mm Hg)	26±2	20±2	41±2	26±3
Cardiac output (liters/min)	6.6±0.3	4.4±0.7	9.2±0.3	5.6±1
Heart rate (beat/min)	63±9	59±11	83±7	71±11
Ventilation (liters/min)	10±3	11±3	20±4	18±9
Saturation (%)	97±1	96±3	86±1	84±4

B Exercise Capacity

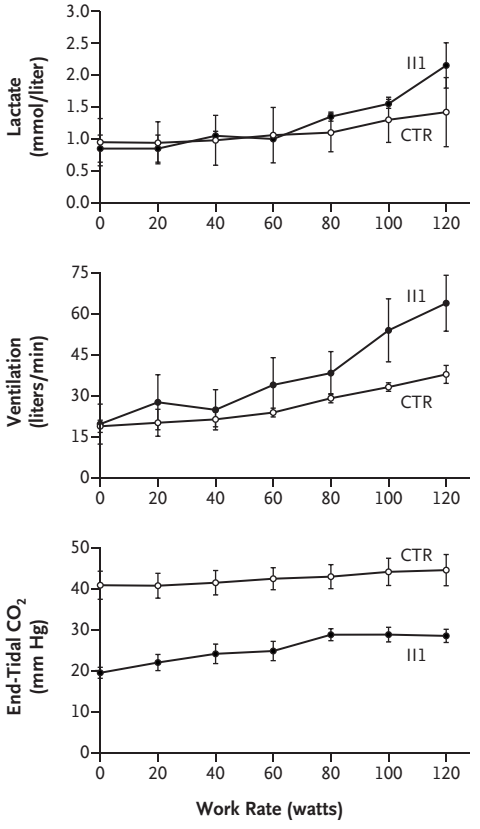

C Gene-Expression Profiles

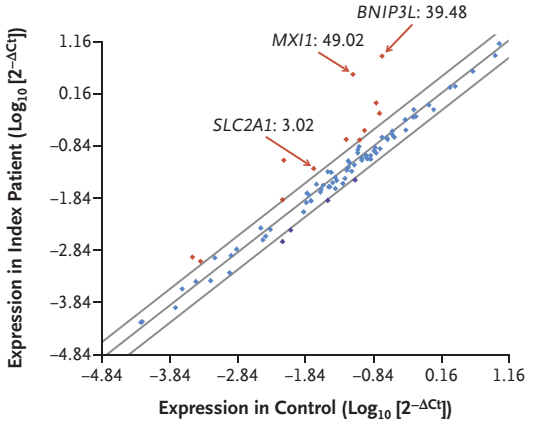

D *BNIP3L* and *MXI1* Transcript Analysis

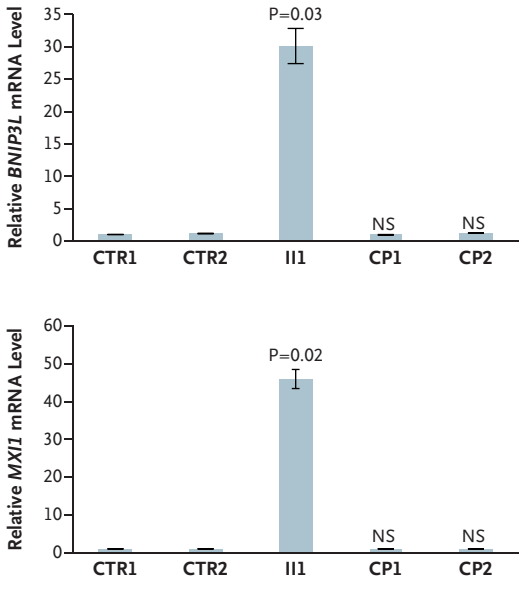

E BNIP3L and MXI1 Protein Analysis

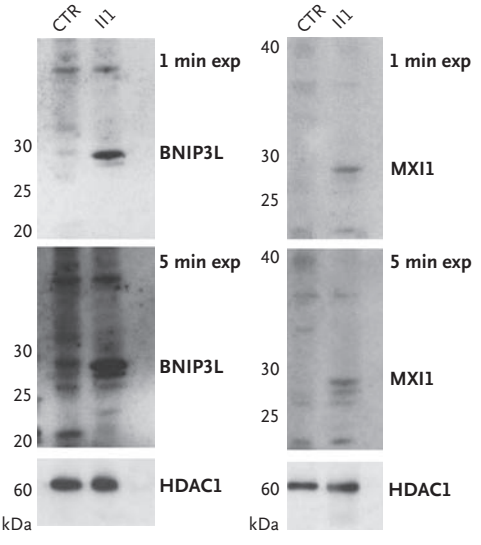

tient's muscle mitochondrial respiratory capacity relative to that in a control (Fig. 3A). The oxidative phosphorylation capacity supported by fatty-acid substrates ($OctM_p$) was 28% lower in the patient, and oxidative phosphorylation capacities supported by substrates for electron transport

The New England Journal of Medicine
Downloaded from nejm.org at the Bodleian Libraries of the University of Oxford on March 4, 2020. For personal use only. No other uses without permission.
Copyright © 2020 Massachusetts Medical Society. All rights reserved.

Figure 2 (facing page). Exercise Capacity and Gene Expression.

Panel A shows the mean (±SD) end-tidal partial pressure of oxygen and carbon dioxide, cardiac output, heart rate, ventilation, and saturation at baseline and in response to acute exposure to hypoxia in the patient and in healthy controls. Pulmonary arterial systolic pressure (PASP) values are shown for 15 healthy control participants. Panel B shows lactate concentration, ventilation, and end-tidal partial pressure of carbon dioxide as a function of work rate on the cycle ergometer; the values for the patient (II1) are minute means and standard deviations (I bars) recorded over the course of two tests. The results for 6 healthy controls are shown for comparison; controls stopped exercising later in the protocol (mean maximal work rate, 240 watts; data not shown). Panel C shows gene-expression profiles of several hypoxia-related genes, evaluated with a comprehensive RT-PCR array in patient PBMC total RNA and shown as a scatterplot of data for the patient and a control (from three independent experiments). ΔCt is the difference between the cycle threshold for the gene of interest and the mean cycle threshold from five reference genes. Red data points indicate genes with significantly higher expression in the patient than in the control, and purple data points indicate genes with significantly lower expression in the patient than in the control; expression of the genes indicated by blue data points did not differ significantly between the patient and the control. The genes with the largest deviation from the control were *BNIP3L* and *MXI1*. *SLC2A1* (encoding GLUT1, a glucose transporter) is also highlighted, since this gene has been studied in relation to the metabolism of glucose. Numbers shown next to these three genes are the estimated ratio of expression in the patient to expression in the control. *BNIP3L* and *MXI1* transcripts (Panel D) were quantified in two controls (CTR1 and CTR2), the patient (II1), and two patients with Chuvash polycythemia (CP1 and CP2) by RT-qPCR performed on PBMC total mRNA. The mRNA levels were normalized to a standard (β-actin). The results are the means and standard deviations (I bars) of three independent evaluations. The P value is for the comparison with control; NS denotes no significant difference. Panel E shows levels of both BNIP3L and MXI1 proteins, analyzed by Western blot in PBMC protein extracts from the control (CTR) and the patient (II1); levels of these proteins were higher in the patient than in the control. Histone deacetylase 1 (HDAC1) was used as a control for equal loading.

chain complex I (GM_P) and for complexes I and II in combination (GMS_P) were 44% and 34% lower, respectively. LEAK respiration (i.e., oxygen consumption in the absence of ATP synthesis [$OctM_L$]) per unit muscle mass did not differ; however, it was 31% higher when expressed relative to electron transport chain capacity, with LEAK respiration making up a greater proportion of total oxygen consumption. Together, these data indicate that the patient's muscle mitochondrial respiratory capacity was substantially low, but with greater LEAK respiration per mitochondrial unit, which suggests that there was uncoupling of oxygen consumption from ATP production. The suppression of mitochondrial respiratory capacity and fatty-acid oxidation resembles that seen in healthy humans acclimatizing to high-altitude hypoxia.[26] Electron microscopy revealed that the patient had high levels of unusual intermitochondrial connecting ducts (similar to cardiac nanotunnels) extending from mitochondria in a direction perpendicular to the long axis of the fiber (Fig. 3B). These ducts have been observed only in mitochondrial myopathy[27,28] and, to a much lesser extent, in normal muscle.[29] They can form an extensive network for physiological exchanges, possibly contributing to mitochondrial survival under stress conditions.

GLUCOSE AND LIPID METABOLISM

We investigated the patient's glucose and lipid metabolism in light of the metabolic shift from oxidative phosphorylation to glycolysis associated with *VHL* loss of function. GLUT-1, a uniporter supporting cellular glucose entry that is under transcriptional control by HIF-1α, was increased at the RNA and protein levels (Fig. S1F and S1G). Metabolomic analysis of muscle tissue highlighted that levels of almost all glycolytic intermediates were substantially lower in the patient than in the control (by 81 to 98%) (Table 2). Low levels of glycolytic metabolites in association with increased GLUT-1 and high levels of circulating lactate suggest that glucose utilization by muscle was enhanced, which accounts for the remarkable venous hypoglycemia (Table 1). Patients with familial erythrocytosis type 2 have been described as having a lower mean blood glucose level than controls, albeit still within the physiologic range, with the lower quartile of patients having glucose levels lower than 56 mg per deciliter (3.1 mmol per liter).[30] The levels of all tricarboxylic acid cycle intermediates (from α-ketoglutarate to malate) were reduced in the index patient's muscle, alongside slightly higher levels of citrate and isocitrate than in the control and an oxaloacetate level that was 10 times as high as in the control (Fig. S2A). The difference in oxaloacetate levels could result from altered aspartate metabolism and might explain the elevated citrate levels. High cellular citrate and oxaloacetate levels might also originate from increased

The New England Journal of Medicine
Downloaded from nejm.org at the Bodleian Libraries of the University of Oxford on March 4, 2020. For personal use only. No other uses without permission.
Copyright © 2020 Massachusetts Medical Society. All rights reserved.

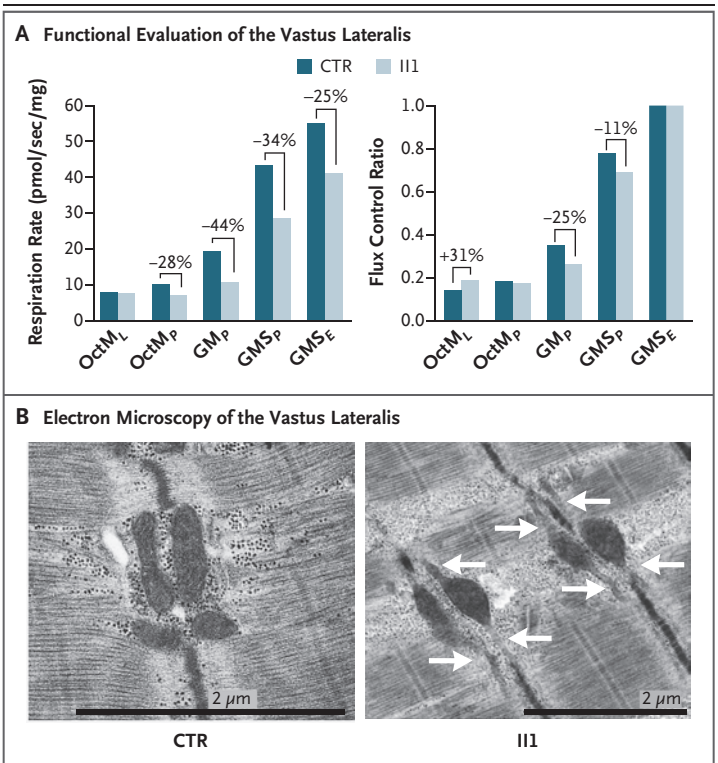

Figure 3. Effects of Low Levels of VHL on Mitochondrial Respiratory Activity.

Panel A shows a functional evaluation of vastus lateralis biopsy specimens; on the left, the mitochondrial respiration rates are corrected for the wet mass of muscle and include LEAK state respiration (i.e., oxygen consumption in the absence of ATP synthesis) with malate and octanoyl carnitine ($OctM_L$); oxidative phosphorylation (OXPHOS)–state respiration with malate and octanoyl carnitine ($OctM_P$); OXPHOS-state respiration through the N pathway by complex I with glutamate and malate (GM_P); OXPHOS-state respiration through NS pathways by complex I and II with glutamate, succinate, and malate (GMS_P); and electron transport chain capacity by titration of the mitochondrial uncoupler FCCP (GMS_E). On the right, the respiratory states are instead corrected for GMS_E. Data are the means obtained from duplicate experiments on the same muscle-biopsy specimen in both a control and the patient. Differences are shown above the bars as percentages. Panel B shows a transmission electron microscopy analyses of vastus lateralis–biopsy specimens from a control (CTR) and the patient (II1). The image on the right shows mitochondrial extensions (arrows). These extensions are larger than T tubules and are located at the same level as mitochondria bodies, on either side of the Z line and in close proximity to it. They provide direct continuity between mitochondria and are not associated with a triad.

Table 2. Metabolomic Data.*

Metabolite or Amino Acid	Ratio (Patient:Control)
Metabolites	
Glucose-6-phosphate	0.05
Fructose-6-phosphate	0.05
Fructose 1,6-bisphosphate	0.12
Glyceraldehyde-3-phosphate	0.16
Dihydroxyacetone phosphate	0.12
Bisphosphoglycerate	1.22
2- and 3-Phosphoglycerate	0.14
Phosphoenolpyruvate	0.19
Pyruvate	0.02
Amino acids	
Ornithine	0.22
Asparagine	0.16
Aspartate	0.44
Glutamine	0.15
Glutamate	0.30
Proline	0.20
Valine	0.22
Isoleucine	0.26
Leucine	0.26

* Metabolomic data were obtained by ultra-high-performance liquid chromatography–mass spectrometry of extracts derived from biopsy specimens of the vastus lateralis. Data obtained for each glycolytic metabolite and amino acid were normalized to the total protein levels and are shown as ratios (patient:control).

glutamine metabolism, as has been observed in patients with VHL deficiency. Lower levels of all amino acids studied were seen, possibly because of their consumption as a carbon source for energy metabolism (Table 2). Muscle ATP levels and energy charge (a marker of the energy status of the tissue) were substantially lower (79%) in the patient, and the phosphocreatine level was 24% lower. The ratio of oxidized to reduced glutathione was 2.44 times as high in the patient, which suggested greater in vivo oxidative stress (Fig. S2B).

Lipid metabolism was evaluated in blood. The patient had low levels of high-density lipoprotein (HDL) cholesterol (Table 1), with a total:HDL cholesterol ratio that suggested a low risk of ischemic heart disease.[31] Low cholesterol levels may be related to the HIF-dependent activation of *INSIG2* (insulin induced gene 2) expression. INSIG2 is a key negative regulator of fatty acids and cholesterol biosynthesis[32] and directly induces degradation of β-hydroxy-β-methylglutaryl-CoA reductase.[33] This up-regulation was not observed in patients with Chuvash polycythemia (Fig. S2C) or any other human disease.

As compared with healthy persons,[34] the patient's fatty-acid distribution in whole blood showed lower levels of monounsaturated fatty

The New England Journal of Medicine
Downloaded from nejm.org at the Bodleian Libraries of the University of Oxford on March 4, 2020. For personal use only. No other uses without permission.
Copyright © 2020 Massachusetts Medical Society. All rights reserved.

acids, especially palmitoleic acid (C16:1) and oleic acid (C18:1), and an arachidonic acid:eicosapentaenoic acid ratio that was 4 times as high (Fig. S2D), suggesting increased inflammation in the patient.[35] No substantial difference in circulating malondialdehyde was observed between the patient and controls (Fig. S2E), implying that there was not a substantial degree of lipid peroxidation. Red-cell membranes in the patient had altered lipid compositions (Fig. S2F), which could lead to increased deformability and decreased aggregation and thrombotic risk.

DISCUSSION

The increase in HIF levels caused by *VHL* loss of function, due to either hereditary or acquired mutations, underpins a large spectrum of diseases with different features. Classic VHL syndrome, which is generally caused by hereditary allele inactivation plus a tissue somatic mutation, is characterized by the occurrence of cancers and increased expression of genes, including *VEGF*, that allow tumor development and progression. In contrast, hereditary *VHL* missense mutations can result in erythrocytosis associated with a variety of generally mild symptoms, without development of cancers,[17] as is seen with the R200W mutation, which is endemic in the Chuvash region (Russia) and in Ischia (Italy).[36,37]

Molecular and clinical studies highlighted differences between the index patient and patients with canonical familial erythrocytosis type 2 carrying the R200W homozygous mutation. Homozygosity for the c.222C→A mutation was associated with a severe, congenital decrease in functionally normal VHL, along with a novel pleiotropic syndrome characterized by a reduced growth rate, hypotension, persistent hypoglycemia, erythrocytosis from birth, limited exercise capacity, and marked metabolic alterations, including reduced oxidative phosphorylation capacity. Studies in animal models showed that HIF up-regulation impairs the GH–IGF1 axis, affecting growth rate and down-regulating *IGFBP3* mRNA expression.[38] In our patient, the robust HIF activation might have altered the GH–IGF1 axis, causing a reduction in the growth rate. GH–IGF1 impairment was confirmed by decreased *IGFBP3* mRNA and by the positive effect of IGF1 treatment on growth rate.

Many additional clinical features are likely to be related to altered skeletal-muscle metabolism. Our patient has greatly reduced mitochondrial respiratory capacity, probably as a consequence of HIF-dependent gene expression. Although HIF-related transcriptome analysis (confirmed at the protein level) revealed a high level of promitophagy signals, muscle mitochondrial density (as opposed to respiratory capacity) was unaffected, in contrast to findings in adapted Tibetan highlanders.[26]

Electron microscopy revealed that muscle mitochondria had an unexpectedly high number of microtubular extensions, which were clearly connected to mitochondria at both ends and thus allowed equilibrium of membrane potential and exchange of solutes over long distances. These structures create a dynamic communication network, potentially contributing to mitochondrial survival under conditions of stress by counteracting autophagic stimuli.

Phlebotomy to reduce erythrocytosis causes iron deficiency, which can alter energy metabolism.[39] In our patient, long-term iron supplementation was sufficient to partially restore concentrations of non–transferrin-bound iron and ferritin, which were higher than in patients with Chuvash polycythemia (median ferritin level, 14 ng per milliliter among 24 patients) with mildly altered gene expression.[22] The mitochondrial abnormalities observed in our patient are distinct from those in patients with iron deficiency,[40] which only mildly reduces the lactate threshold in humans. The unique, complex clinical phenotype observed in our patient might arise from the mitochondrial dysfunction, other deregulated pathways, and, probably, as-yet-undescribed adaptive mechanisms.

We conclude that this newly identified syndrome is a direct demonstration of the exquisitely sensitive interaction between VHL and HIF in the regulation of human metabolism and skeletal-muscle function.

Supported by a grant from the Associazione Italiana Ricerca sul Cancro (11653, to Dr. Della Ragione), Programma VALERE, Vanvitelli per la Ricerca (to Dr. Bencivenga and Ms. Caiazza), 2015 Campania Regional funding for rare diseases (to Dr. Perrotta), the Evelyn Trust (to Dr. Murray), and King's College London, University of Oxford, and the Physiological Society (to Dr. Formenti).

Disclosure forms provided by the authors are available with the full text of this article at NEJM.org.

We thank the patient and his family for their participation in and assistance with the study; and Eva Franziska Graber and Hans Hoppeler (University of Bern, Switzerland), Stefan J.A. Buk (King's College Hospital, London), and Keith L. Dorrington (University of Oxford, Oxford) for helpful discussions.

The New England Journal of Medicine
Downloaded from nejm.org at the Bodleian Libraries of the University of Oxford on March 4, 2020. For personal use only. No other uses without permission.
Copyright © 2020 Massachusetts Medical Society. All rights reserved.

REFERENCES

1. Schofield CJ, Ratcliffe PJ. Oxygen sensing by HIF hydroxylases. Nat Rev Mol Cell Biol 2004;5:343-54.
2. Wenger RH. Cellular adaptation to hypoxia: O2-sensing protein hydroxylases, hypoxia-inducible transcription factors, and O2-regulated gene expression. FASEB J 2002;16:1151-62.
3. Maxwell PH, Wiesener MS, Chang GW, et al. The tumour suppressor protein VHL targets hypoxia-inducible factors for oxygen-dependent proteolysis. Nature 1999; 399:271-5.
4. Lenglet M, Robriquet F, Schwarz K, et al. Identification of a new *VHL* exon and complex splicing alterations in familial erythrocytosis or von Hippel-Lindau disease. Blood 2018;132:469-83.
5. Gossage L, Eisen T, Maher ER. VHL, the story of a tumour suppressor gene. Nat Rev Cancer 2015;15:55-64.
6. Maher ER, Neumann HP, Richard S. Von Hippel-Lindau disease: a clinical and scientific review. Eur J Hum Genet 2011; 19:617-23.
7. Kanno H, Kondo K, Ito S, et al. Somatic mutations of the von Hippel-Lindau tumor suppressor gene in sporadic central nervous system hemangioblastomas. Cancer Res 1994;54:4845-7.
8. Young AC, Craven RA, Cohen D, et al. Analysis of VHL gene alterations and their relationship to clinical parameters in sporadic conventional renal cell carcinoma. Clin Cancer Res 2009;15:7582-92.
9. Ang SO, Chen H, Hirota K, et al. Disruption of oxygen homeostasis underlies congenital Chuvash polycythemia. Nat Genet 2002;32:614-21.
10. Bento C, Percy MJ, Gardie B, et al. Genetic basis of congenital erythrocytosis: mutation update and online databases. Hum Mutat 2014;35:15-26.
11. Sarangi S, Lanikova L, Kapralova K, et al. The homozygous VHL(D126N) missense mutation is associated with dramatically elevated erythropoietin levels, consequent polycythemia, and early onset severe pulmonary hypertension. Pediatr Blood Cancer 2014;61:2104-6.
12. Percy MJ, Rumi E. Genetic origins and clinical phenotype of familial and acquired erythrocytosis and thrombocytosis. Am J Hematol 2009;84:46-54.
13. Sergueeva A, Miasnikova G, Lisina E, et al. Thrombotic complications are associated with phlebotomy therapy in patients with Chuvash polycythemia. Blood 2015; 126:936. abstract.
14. McMullin MFF, Mead AJ, Ali S, et al. A guideline for the management of specific situations in polycythaemia vera and secondary erythrocytosis: a British Society for Haematology Guideline. Br J Haematol 2019;184:161-75.
15. Solomon EI, Decker A, Lehnert N. Non-heme iron enzymes: contrasts to heme catalysis. Proc Natl Acad Sci U S A 2003;100:3589-94.
16. Richards S, Aziz N, Bale S, et al. Standards and guidelines for the interpretation of sequence variants: a joint consensus recommendation of the American College of Medical Genetics and Genomics and the Association for Molecular Pathology. Genet Med 2015;17:405-24.
17. Gordeuk VR, Sergueeva AI, Miasnikova GY, et al. Congenital disorder of oxygen sensing: association of the homozygous Chuvash polycythemia VHL mutation with thrombosis and vascular abnormalities but not tumors. Blood 2004;103:3924-32.
18. Formenti F, Constantin-Teodosiu D, Emmanuel Y, et al. Regulation of human metabolism by hypoxia-inducible factor. Proc Natl Acad Sci U S A 2010;107:12722-7.
19. Smith TG, Brooks JT, Balanos GM, et al. Mutation of von Hippel-Lindau tumour suppressor and human cardiopulmonary physiology. PLoS Med 2006;3(7): e290.
20. Slingo ME, Turner PJ, Christian HC, Buckler KJ, Robbins PA. The von Hippel-Lindau Chuvash mutation in mice causes carotid-body hyperplasia and enhanced ventilatory sensitivity to hypoxia. J Appl Physiol (1985) 2014;116:885-92.
21. Sable CA, Aliyu ZY, Dham N, et al. Pulmonary artery pressure and iron deficiency in patients with upregulation of hypoxia sensing due to homozygous VHL(R200W) mutation (Chuvash polycythemia). Haematologica 2012;97:193-200.
22. Zhang X, Zhang W, Ma SF, et al. Iron deficiency modifies gene expression variation induced by augmented hypoxia sensing. Blood Cells Mol Dis 2014;52:35-45.
23. Baxter RC. Insulin-like growth factor binding protein-3 (IGFBP-3): novel ligands mediate unexpected functions. J Cell Commun Signal 2013;7:179-89.
24. Bellot G, Garcia-Medina R, Gounon P, et al. Hypoxia-induced autophagy is mediated through hypoxia-inducible factor induction of BNIP3 and BNIP3L via their BH3 domains. Mol Cell Biol 2009;29: 2570-81.
25. Corn PG, Ricci MS, Scata KA, et al. Mxi1 is induced by hypoxia in a HIF-1-dependent manner and protects cells from c-Myc-induced apoptosis. Cancer Biol Ther 2005;4:1285-94.
26. Horscroft JA, Kotwica AO, Laner V, et al. Metabolic basis to Sherpa altitude adaptation. Proc Natl Acad Sci U S A 2017; 114:6382-7.
27. Vincent AE, Ng YS, White K, et al. The spectrum of mitochondrial ultrastructural defects in mitochondrial myopathy. Sci Rep 2016;6:30610.
28. Vincent AE, Turnbull DM, Eisner V, Hajnóczky G, Picard M. Mitochondrial nanotunnels. Trends Cell Biol 2017;27: 787-99.
29. Vincent AE, White K, Davey T, et al. Quantitative 3D mapping of the human skeletal muscle mitochondrial network. Cell Rep 2019;27:321.
30. McClain DA, Abuelgasim KA, Nouraie M, et al. Decreased serum glucose and glycosylated hemoglobin levels in patients with Chuvash polycythemia: a role for HIF in glucose metabolism. J Mol Med (Berl) 2013;91:59-67.
31. Lemieux I, Lamarche B, Couillard C, et al. Total cholesterol/HDL cholesterol ratio vs LDL cholesterol/HDL cholesterol ratio as indices of ischemic heart disease risk in men: the Quebec Cardiovascular Study. Arch Intern Med 2001;161:2685-92.
32. Yabe D, Brown MS, Goldstein JL. Insig-2, a second endoplasmic reticulum protein that binds SCAP and blocks export of sterol regulatory element-binding proteins. Proc Natl Acad Sci U S A 2002; 99:12753-8.
33. Hwang S, Nguyen AD, Jo Y, Engelking LJ, Brugarolas J, DeBose-Boyd RA. Hypoxia-inducible factor 1α activates insulin-induced gene 2 (Insig-2) transcription for degradation of 3-hydroxy-3-methylglutaryl (HMG)-CoA reductase in the liver. J Biol Chem 2017;292:9382-93.
34. Rizzo AM, Montorfano G, Negroni M, et al. A rapid method for determining arachidonic:eicosapentaenoic acid ratios in whole blood lipids: correlation with erythrocyte membrane ratios and validation in a large Italian population of various ages and pathologies. Lipids Health Dis 2010;9:7.
35. Simopoulos AP. The importance of the ratio of omega-6/omega-3 essential fatty acids. Biomed Pharmacother 2002; 56:365-79.
36. Sergeyeva A, Gordeuk VR, Tokarev YN, Sokol L, Prchal JF, Prchal JT. Congenital polycythemia in Chuvashia. Blood 1997;89:2148-54.
37. Perrotta S, Nobili B, Ferraro M, et al. Von Hippel-Lindau-dependent polycythemia is endemic on the island of Ischia: identification of a novel cluster. Blood 2006;107:514-9.
38. Kartal Ö, Aydınöz S, Kartal AT, et al. Time dependent impact of perinatal hypoxia on growth hormone, insulin-like growth factor 1 and insulin-like growth factor binding protein-3. Metab Brain Dis 2016;31:827-35.
39. Dziegala M, Josiak K, Kasztura M, et al. Iron deficiency as energetic insult to skeletal muscle in chronic diseases. J Cachexia Sarcopenia Muscle 2018;9:802-15.
40. Hoes MF, Grote Beverborg N, Kijlstra JD, et al. Iron deficiency impairs contractility of human cardiomyocytes through decreased mitochondrial function. Eur J Heart Fail 2018;20:910-9.

Copyright © 2020 Massachusetts Medical Society.

The New England Journal of Medicine
Downloaded from nejm.org at the Bodleian Libraries of the University of Oxford on March 4, 2020. For personal use only. No other uses without permission.
Copyright © 2020 Massachusetts Medical Society. All rights reserved.